

The unique physical properties of the hydrogen bonded in dimers liquid crystals

M Petrov, B Katranchev and P M Rafailov

Institute of Solid State Physics, Bulgarian Academy of Sciences, 72 Tzarigradsko
Chaussee Blvd., 1784 Sofia, Bulgaria.

E-mail: mpetrov@issp.bas.bg

Abstract. The dimerization of aromatic carboxylic acids, is the base of the structure formation of hydrogen bonded in dimers liquid crystals (HBDLCs), that exhibit non-conventional mesomorphism. The structural units of these LCs are amphiphilic-type molecules, which after suitable functionalization, induce supramolecular complexes, nanocomposites based on HBDLCs. The liquid crystalline character of the nanocomposites strongly dependent on intermolecular hydrogen bonds between symmetric, where the H-donors and H acceptors are contained in similar and non-symmetric HBDLCs, where the H-donors and H acceptors are contained in unlike molecules. The strength and non-covalent character of the hydrogen bonds provides both sufficient HBDLCs complex stability and bonding flexibility with a possibility to design and drive the supramolecular geometry. We investigated a series of nanocomposites produced by mixture of HBDLC (*p*-*n*-alkyloxybenzoic acid - nOBA), serving as matrices, with non-mesogenic (single walled carbon nanotubes - SWCNTs, hydroxypyridine – HOPY) and mesogenic (cholesteryl benzoate - ChB) nano-particles in various shapes and sizes. A set of new chiral ferroelectric phases were found in the nanocomposites, otherwise do not appearing in the pristine achiral HBDLCs materials. A molecular model of an unique low-temperature ferroelectric smectic phase C based on the molecular dimer ring symmetry reduction (bent dimer formation) towards to the lowest triclinic one is presented for both symmetric and nonsymmetric supramolecular liquid crystal complexes.

1. Introduction

The hydrogen bond (HB) enables various mesogenic and non-mesogenic compounds to form complexes exhibiting rich-phase polymorphism. It is an efficient alternative to covalent bonding as a way to stabilise liquid crystallinity. This bonding yields symmetric and non-symmetric complexes hydrogen bonded dimer liquid crystals (HBDLCs). HBDLCs are composed of a proton donor and acceptor molecules. Usually, for formation of HBDLCs, the carboxylic acids are preferable [1,2]. Thus, as part of a systematic development of this area the relationships between the phase behaviour and hydrogen bonding in a series of *p*-*n*-alkyloxybenzoic acids (nOBA) is an important LC topic.

The *p*-*n*-alkyloxybenzoic acid (nOBA) LCs are the basic components in forming supramolecular systems [3]. The strong ability to conformation of the dimeric structure in the principally achiral nOBAs creates the possibility for emergence of induced chirality [4]. The liquid crystalline nature of alkyloxybenzoic acids keeps at mixing with mesogenic or non-mesogenic compounds due to the hydrogen bonding. This non-covalent interaction predetermines the physical properties of nOBA LCs.

Due to the properties of the hydrogen bond, namely: directionality, reversibility and specificity, a wide range of homomeric and heteromeric complexes have been prepared exhibiting diversity of new electrooptical properties [4]. The non-symmetric supramolecular compound are complexes favoured

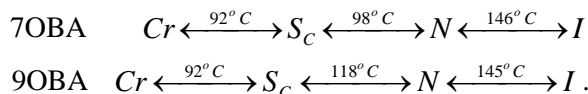


by the stronger hydrogen bond between unlike units, while the symmetric ones exhibit such interaction between equivalent components. So, the formation of heteromeric complexes are mixtures of dissimilar H-donors and H-acceptors. A wide class of supramolecular liquid crystals was obtained by mixture of dimeric liquid crystals with set of non-mesogenic or mesogenic nanoparticles with different sizes and shapes [4]. In such produced composite states, the liquid crystal serves as a matrix with ability to impose its inherent high ordering to the bulk ordering of the mixture. Carbon nanotubes are among the most used as doping agent in the liquid crystal matrix [5-7].

The goal of the present work is to create both symmetric and non-symmetric supramolecular liquid crystals complexes, nanocomposites, where the dimeric nOBA liquid crystal serves like matrix. To produce the symmetric supramolecular liquid crystals complexes we use the dimeric LC 7OBA, mixed with SWCNTs and for non-symmetric nanocomposites we mix the dimeric LCs, 9OBA with mesogenic, cholesteryl benzoate (ChB) or non-mesogenic 4, hydroxypyridine (HOPY) nanoparticles, aiming to detect and explain the mechanism of induction of chirality and ferroelectricity, smectic C_G phase respectively, in the symmetric and non-symmetric nanocomposites. In order to understand the mechanism of the dimer ring bending, leading to symmetry decrease and C_G phase induction both in symmetric and non-symmetric complexes we present a balance of the intra and inter-molecular forces created by hydrogen bonding, and electrostatic (dipole moments) interactions.

2. Experimental results and discussion

2.1. For the symmetric nanocomposites we used 7OBA supplied by Sigma-Aldrich (Product of Japan) with strength of the linear hydrogen bond $20 \text{ kJ}\cdot\text{mol}^{-1}$, which is two times bigger than those of 9OBA ($\approx 10 \text{ kJ}\cdot\text{mol}^{-1}$). The phase transitions temperatures of pristine 7,9OBA are:



We examined the mixture 7OBA/SWCNTs with SWCNT concentration $c = 0.01 \text{ wt}\%$ which was found to be optimal for the induction of chiral and ferroelectric states [8]. Purified SWCNT with diameters in the range 1.2–1.4 nm and an aspect ratio of 20–2000, assembled in thin bundles of $>2 \mu\text{m}$ length, produced by arc discharge at Hanwha NanoTech Co., Ltd., were used as purchased. For the microtextural polarization analysis we used the known liquid crystal cell (LCC), two glass plates covered with ITO rubbed layer and the sample thickness $d=8 \mu\text{m}$. As was indicated in [8,9] the chiral induction in the nanocomposite was more effective due to both thin cell and good orientation in accordance with an optimal concentration. This effect determines the choice of these experimental parameters. We recall (see [8]) that at these experimental conditions the induced chiral and ferroelectric states at cooling are: $I \rightarrow N$, $N \rightarrow N^*$, $S_C^* \rightarrow N_r^*$, $N_r^* \rightarrow C_G$, where N^* - chiral nematic, S_C^* - ferroelectric smectic C, N_r^* - reentrant chiral nematic and C_G - low temperature smectic C_G state. We concentrate on the low-temperature smectic C_G state, which appears at 86°C at cooling. The microtexture of the produced smectic C_G state in the symmetric supramolecular nanocomplex 7OBA/SWCNT is indicated in figure 1. We remind that the nanocomposite, created in such way is symmetric, since the dimer ring binds two similar molecules (the two monomers) by two parallel linear hydrogen bonds.

The microtextural characteristics, equal left- and right-handed helices figure 1, are evidence for chirality and biaxiality of the LC mixture. Thus, the dimeric LC 7OBA/SWCNTs mixture, at cooling from I phase, exhibits consecutive local molecular symmetry reductions, leading to macroscopical one with the lowest triclinic symmetry C_1 (smectic C_G) where none of the principle axes of the second rank tensor, characterizing the orientational order, makes an angle of 0° or $\pi/2$ with the smectic layer's planes [10]. This strong local molecular symmetry decrease, can be realized only, when a local polarization induced by dimer conformation, or polar vector \mathbf{P} bound up with the LC director \mathbf{n} , points out of the smectic layer's planes, thus the ground characteristic of the smectic C_G phase. Our microtexture and thermal analyses thus hint at a bent form of the dimer ring of 7OBA in the presence of the SWCNTs.

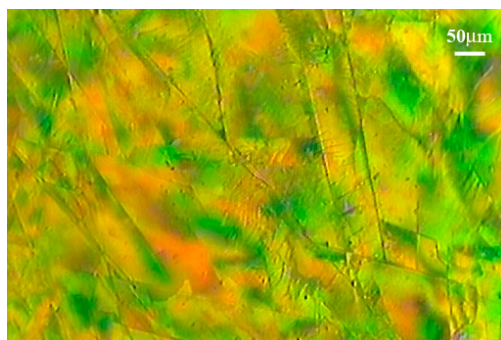


Figure 1. Colored mosaic C_G texture with equal left- and right-handed helices.

2.2. For the produce of the non-symmetric nanocomposites, we mix first the mesogenic nanocomponent ChB with 9OBA (9OBA/ChB) and second the non-mesogenic HOPY with 9OBA (9OBA/HOPY).

We recall that in the non-symmetric nanocomposite (non-symmetric supramolecular LC complex) the dimer ring of the dimeric LC is in the open state (open dimer) where the one free hydrogen bond, serving as H-bond donor, bind with free O atom (H-bond acceptor) of the nanoparticle. This means that the typical dimer symmetry, characterizing the pristine nOBA LC is destroyed and the symmetry of the complex is reduced. As we indicate in the figure 2 the smectic C_G phase is also induced in these cases, with textures strongly discernable from that of the symmetric 7OBA/SWCNTs complex. This difference hints for two different mechanisms for the C_G phase induction. Any more it indicates the unique role of the hydrogen bonding for build and design of nanocomposites.

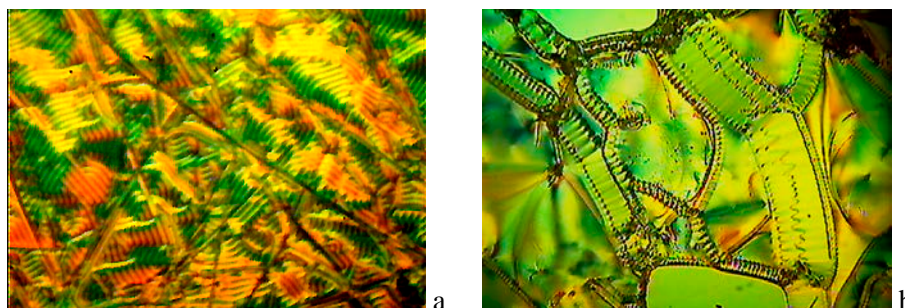


Figure 2. (a) The C_G texture of the nanocomposite 9OBA/ChB. (b) The C_G texture of the nanocomposite 9OBA/HOPY.

At this stage of discussion one notes, that the C_G microtextures of 9OBA/ChB and 9OBA/HOPY, to some extent, resemble those of the high-molecular bent-core C_G textures, which start to develop at cooling down to solid state, but without reaching a thermodynamical equilibrium. We designate such forming C_G phase as a developable. Contrary, the C_G phase texture of the symmetric nanocomposite 7OBA/SWCNTs was observed as stable and permanent with respect to the mosaic domains formation during the cooling down to the solid state. We designate such forming C_G phase as a developed.

In order to develop a model and corresponding mechanism of induction of C_G phase, both in symmetric and nonsymmetric supramolecular nanocomplexes, exposed by developed and developable C_G states, we use some characteristic for the pristine nOBA matrix parameters obtained on the base of the chemical AB INITIO MO calculation [11] and x-ray analysis [12]. The evolution of the hydrogen bonds of nOBA at cooling is indicated in [8,9]. Due to the thermal action, without external excitations, the symmetric dimer ring evolutes consequently to open dimer and oligomer (restricted polymer), but finally the system remains LC noncomposite. Thus in the combination with SWCNTs there is no

chemical bond with external unsimilar molecule as that of the nanoparticle. For that case the characteristic geometrical and energetic parameter are as follows [11,12]: The geometrical parameters are for the monomer r inter-atom distances r : $r_{C=O}=1.2202\text{\AA}$, $r_{C-O}=1.3934\text{\AA}$, $r_{O-H}=0.9896\text{\AA}$, angle $\gamma_{O-C=O}=121.26^\circ$ (angle between C=O and C-O groups); Closed Dimer: $r_{O\dots H}=1.5024\text{\AA}$, $r_{C=O}=1.2385\text{\AA}$, $r_{C-O}=1.3521\text{\AA}$, $r_{O-H}=1.0120\text{\AA}$, angle $\gamma_{O-C=O}=123.82^\circ$; Open Dimer: $r_{O\dots H}=1.6761\text{\AA}$, $r_{C=O}=1.2222\text{\AA}$, $r_{C-O}=1.3798\text{\AA}$, $r_{O-H}=0.9942\text{\AA}$, angle $\gamma_{O-C=O}=122.71^\circ$. These parameters depict the disposition of the bonds participating in the vibrational spectra characteristic of the dimer ring. It is seen that there is a small variation of the geometrical parameters of the different molecular forms. Significant difference, however, in the energy and the dipole moment values exists when the three fundamental dimer forms appear. Thus, for 7OBA, the dipole moments μ in D (Debye) are 2.2643D for monomers, 0.0418D for the closed dimer and 4.7716D for the open dimers [11]. The dipole moment value of the closed dimer is approximately zero in accordance with simple logical considerations. In geometrical presentation, this means two approximately equal parallel dipoles with opposite directions. In the physical sense $\mu_{\text{dim}} \approx 0$ reflects the compensative role on μ of the closed dimer formation, implying that the molecule transforms from dipole (monomer) into quadrupole dielectric state. The calculated energies (ΔE) [11] of transition between monomer, closed dimer and open dimer of 7OBA or specially the energy of a linear hydrogen bond in the closed dimer is $1/2\Delta E_{\text{mon}\rightarrow\text{dim}}$ and is $24\text{ kJ}\cdot\text{mol}^{-1}$ in good correspondence with that measured in [13].

The dimer structure $(R-CO-OH)_2$ (figure 3(a)) characterizes with 6 fundamental vibrations, which considered as Cartesian displacements, may be described as hydrogen bond stretching vibrations, in-plane or out-of- plane hydrogen bond bending vibrations or twisting vibrations [14,15]. Nevertheless, the closed dimer molecules are molecular quadrupoles. One can impose a dipole approximation, assuming the positive and the negative charges of the absorbing dimeric LC to segregate, following their distribution centers. In such way the ensemble of dimer molecules is a supra molecular LC system with an equivalent transition dipole moment \mathbf{P} , which can rotate around the C-C molecular axis. This transition dipole moment \mathbf{P} , or equivalent polar vector \mathbf{P} expressing also the polar director, indicating the intra-molecular degree of freedom or conformational order parameter, deviates by an angle from the long molecular axis of the non-excited dimer as shown in figure 3. This figure presents the geometry of the polar vector deviation and depicts the dimer ring bending, quantified by the dimer bending kink vector $\mathbf{m} \sim \mathbf{n}_1 \times \mathbf{n}_2$ where \mathbf{n}_1 and \mathbf{n}_2 are the unit vectors pointing along the two wings of the dimer. As a result, when bending of the dimer ring is present, \mathbf{n}_1 and \mathbf{n}_2 represent two local directors both including angle with the director \mathbf{n}_0 of the initially oriented dimeric LC system. Therefore, this is the geometry depicting the conformational order parameter in the dimeric system conformed by external actions.

Besides this important effect of the vibration softening hinting at dimer bending in the frame of the dimer ring structure, the Raman spectra in the range of $100\text{--}300\text{ cm}^{-1}$ (see [8,9]), also indicate π -stacking interactions between the SWCNT (carbon aromatic hexagon) and the liquid crystal molecule in its benzene core part. In the aspect of the competition between the forces promoted by these intra- and intermolecular interactions, and on the ground of the dominating bending (observed as s IR spectral polarization vibration [13]) one can conclude: that both perpendicular to the molecular optic axis forces are in coordination with the π - π electronic interaction, thus promoting a local molecular bending (bent dimer) and in consequence causing local and macroscopic symmetry decrease. Such local molecular symmetry decreases presume a macroscopic symmetry decrease characteristic for C_g . In the figure 3(b) a possible molecular model of the bulk interaction of the 7OBA LC matrix and the near-by SWCNT structure unit is depicted. H indicates the H-bonding vibration induced by the bending and detected by s IR light polarization. The direction of this s IR vibration is collinear with the stacking Raman vibration modulating the electronic π - π interaction between the LC benzenes and the carbon hexagons of the SWCNTs causing the LC dimer ring to bend and further to promote a multitude of sterically grazed bent dimers. As a result of this nanoscale process, a macroscopic electrical polarization \mathbf{P} arises, which is characteristic of ferroelectric LC states [16,17].

We depict the two mechanisms and corresponding models for symmetric and non-symmetric supramolecular complexes in figure 3 and figure 4. For that purpose we use the above presented geometrical and energetic parameters and by torque balance of the non suppress forces we obtain the resultant, non zero space, vector bending the dimer ring, thus provoking the symmetry reduction to the lowest one triclinic characterizing the found by us smectic C_G phase (figure 3(c)). The polarization vector thus has two components: one is in the layer plane and the other one is an out-of-plane component.

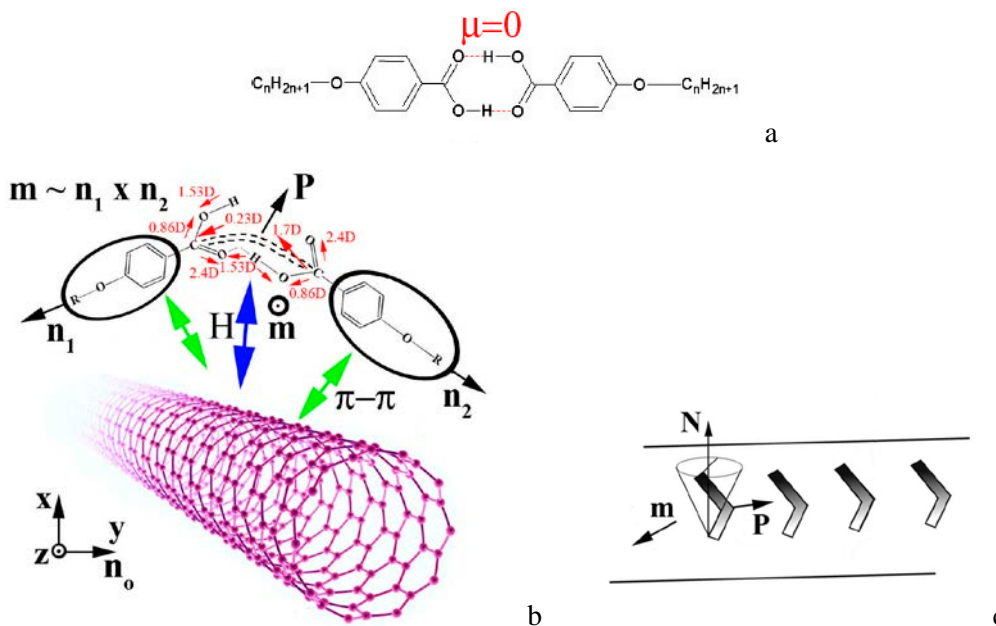


Figure 3. (a) The closed dimer. (b) A molecular model of the symmetric 7OBA/SWCNT nanocomposite. The average hydrogen bond (blue arrow), the $\pi-\pi$ electronic interaction (green arrow) and the multitude of the acting local dipoles (red arrows), all participating in the force balance are indicated. The SWCNT hexagon point z axis. (c) The lowest one triclinic symmetry characterizing the smectic C_G phase.

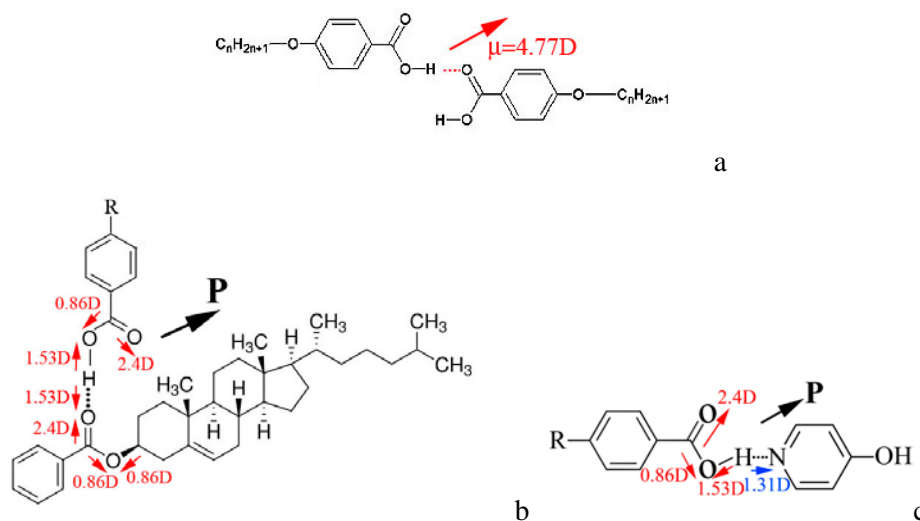


Figure 4. (a) The non-symmetric open dimer. (b) Molecular model of 9OBA/ChB (c). Molecular model of 9OBA/HOPY.

3. Conclusion

The symmetric and non-symmetric supramolecular liquid crystals, nanocomposites, both fulfilled on the base of the hydrogen bonding at mixing of dimeric nOBA liquid crystals with mesogenic or non-mesogenic nanoparticles, significantly differ with respect to generation and development of chiral ferroelectric states, including smectic C_G one. A possible reason for such a difference is that in the non-symmetric nanocomposites, exhibiting developable C_G state, the hydrogen bonding is heteromeric type, able to create non-homogeneous and non-stable in time dimer ring symmetry reduction, thus initiation thermodynamically unstable state. In this sense, the non-symmetric supramolecular liquid crystals, nanocomposites, resemble the high-molecular bent-core liquid crystal complexes. Unlike, in the symmetric supramolecular complexes, like that of 7OBA/SWCNTs, hydrogen bonding develops between two similar molecules, the two monomers of the nOBA molecule, within the electrical and steric field of the doped carbon nanotubes. The interaction of the two similar components of the nanocomposite 7OBA/SWCNTs, evidently leads to a thermodynamically stable developed C_G state. The future experimental and theoretical investigations are directed to further elaboration and confirmation of this model.

Acknowledgments

The work is supported by grant INERA EU project (FP7-316309-REGPOT-2012-2013-1) "Research and Innovation Capacity Strengthening of ISSP-BAS in Multifunctional Nanostructures" and Grant BK-04-14 from the Institute of Solid State Physics, Bulgarian Academy of Sciences.

References

- [1] Kato T and Frechet J M J 2006 *Liquid Crystals* **33** 1429
- [2] Paleos C M and Tsiourvas D 2001 *Liquid Crystals* **28** 1127
- [3] Paterson D A, Martinez-Felipe A, Jansze S M, Marcelis A T M, Storey J M D and Imrie C T 2015 *Liquid Crystals* **42** 928
- [4] Martinez-Felipe A and Imrie C T 2015 *J. Mol. Struct.*, **1100** 429
- [5] Dierking I, Scalia G and Morales P 2005 *J Appl Phys.* **97** 044309
- [6] Taylor J W, Kurihara L K and Martinez-Miranda L J 2012 *Appl Phys Lett.* **100** 173115
- [7] Lynch M D and Patrick D L 2002 *Nano Lett.* **2** 1197
- [8] Petrov M, Katranchev B, Rafailov P M, Naradikian H, Dettlaff-Weglikowska U, Keskinova E and Spassov T 2013 *Phys. Rev. E* **88** 042503
- [9] Katranchev B and Petrov M 2016 *Phase Transitions* **89** 115
- [10] de Gennes P G and Prost J 1993 *The Physics of Liquid Crystals* second edition (New York: Oxford University Press)
- [11] Bobadova-Parvanova P, Parvanov V, Petrov M and Tsonev L 2000 *Cryst. Res. Technol.* **35** 1321
- [12] Bryan R F and Fallon L 1975 *Journal of the Chemical Society-Perkin Transactions* **2** 1175
- [13] Herbert A J 1967 *Trans. Faraday Soc.* **63** 555
- [14] Petrov M, Antonova K, Kirov N, Tenev T and Ratajczak H 1994 *J. Mol. Struct.* **327** 265
- [15] Antonova K, Katranchev B, Petrov M, Marcerou J P, Baran J and Ratajczak H 2004 *J Mol Struct.* **694** 105
- [16] Jakli A, Kruerke D, Sawade H and Heppke G 2001 *Phys Rev Lett.* **86** 5715
- [17] Chattham N, Korblova E, Shao R, Walba D M, MacLennan J E and Clark N A 2010 *Phys Rev Lett.* **104** 067801